Audio Engineering Society

Convention Paper

Presented at the 128th Convention
2010 May 22–25 London, UK

Analysis and Improvement of Pre-equalization in 2.5-Dimensional Wave Field Synthesis

Sascha Spors and Jens Ahrens

Deutsche Telekom Laboratories, Technische Universität Berlin, Ernst-Reuter-Platz 7, 10587 Berlin, Germany

Correspondence should be addressed to Sascha Spors (Sascha.Spors@telekom.de)

ABSTRACT

Wave field synthesis (WFS) is a well established high-resolution spatial sound reproduction technique. Typical WFS systems aim at the reproduction in a plane using loudspeakers enclosing the plane. This constitutes a so-called 2.5-dimensional reproduction scenario. It has been shown that a spectral correction of the reproduced wave field is required in this context. For WFS this correction is known as pre-equalization filter. The derivation of WFS is based on a series of approximations of the physical foundations. This paper investigates on the consequences of these approximations on the reproduced sound field and in particular on the pre-equalization filter. An exact solution is provided by the recently presented spectral division method and is employed in order to derive an improved WFS driving function. Furthermore, the effects of spatial sampling and truncation on the pre-equalization are discussed.

1. INTRODUCTION

Wave Field Synthesis (WFS) is a well established high-resolution spatial sound reproduction technique [1]. It aims at synthesizing the sound field of a desired acoustic scene within a given listening area.

The original theory of WFS considers the reproduction in a planar listening area using a linear distribution of loudspeakers (loudspeaker array). It is assumed that the reproduction in a plane only is suitable for most applications. Typical implementations of WFS systems surround the listening area by piecewise linear or curved loudspeaker arrays. The original theory has been extended in various aspects for this purpose. In this paper we will focus on the traditional concept covering a linear distribution of loudspeakers.

The foundations of WFS are given by the first Rayleigh integral. This integral states that a continuous planar distribution of appropriately driven point sources (secondary sources) is suitable to syn-

thesize any desired sound field within one of the half-spaces bounded by the plane. However, the reproduction in a plane using a linear loudspeaker array is not directly covered by the Rayleigh integral. In WFS, a solution to this problem has been developed by applying a series of approximations to the Rayleigh integral. This results in a driving signal for the loudspeakers that can be split into an loudspeaker position independent pre-equalization filter and a loudspeaker position dependent weighting and delaying of the pre-filtered input signal. However, this approach relies on the validity of the applied approximations and may not be feasible for all situations.

This paper investigates various theoretical and practical aspects in this context and summarizes known results. We will restrict the main findings to linear arrays. However, most of the results will also hold for curved arrays. A previous study by [2] derived a number of findings for the pre-equalization filter of WFS on the basis of numerical simulations. We will complement and extend this study by utilizing an exact solution to the reproduction problem as basis for the analysis of the traditional WFS solution. Furthermore, an improved driving signal has been derived that overcomes some of the shortcomings of WFS.

This paper is organized as follows: We first review the theory of sound field synthesis on basis of the Rayleigh integrals in Section 2. This will serve as a basis for a short review of the traditional derivation of the driving signals in WFS, as presented in Section 3. Special attention will be drawn to the conditions under which the applied approximations are valid. Section 4 introduces the spectral division method (SDM) which serves as a reference solution to the considered reproduction problem. The driving signal for a virtual point source is derived, as well as, the connections of the SDM to WFS. The accuracy of WFS is then evaluated in Section 5 considering critical parameters and scenarios. It is shown that WFS exhibits a number of shortcomings than can be improved by a novel driving signal. Practical realizations of WFS systems are realized by a finite number of loudspeakers. This implies a spatial sampling and truncation of the continuous secondary source distribution assumed so far. The well documented sampling theory for linear WFS systems is reviewed in Section 6 and the consequences on the pre-equalization filter are discussed. Similar considerations follow for the discussion of spatial truncation in Section 7. Finally, a number of conclusions are drawn for the practical aspects of the pre-equalization filter in Section 8.

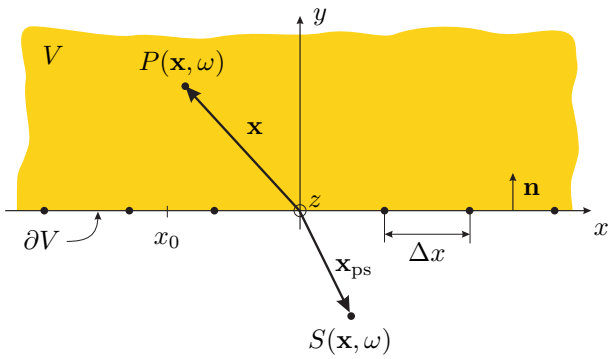

Fig. 1: Geometry underlying the derivation of WFS and the SDM. The reproduction of a virtual point source placed at $\mathbf{x}_{\mathrm{ps}}$ using a linear distribution ∂V of secondary point sources located on the x-axis is considered. The yellow area V denotes the listening area, the z-axis points out of the illustration plane.

2. THEORY OF SOUND FIELD SYNTHESIS

The following section introduces in brief the theory of sound field synthesis for linear/planar loudspeaker arrays. For a more detailed treatment refer to [3, 4, 5, 6].

2.1. The Rayleigh Integrals

Without loss of generality, the geometry depicted in Fig. 1 will underly the considerations of this paper. The acoustic pressure $P(\mathbf{x},\omega)$ within the half-space V is given by the first Rayleigh integral [7]

$$P(\mathbf{x},\omega) = 2 \iint_{-\infty}^{\infty} \frac{\partial}{\partial \mathbf{n}} P(\mathbf{x}_0,\omega)\, G_{0,3\mathrm{D}}(\mathbf{x}|\mathbf{x}_0,\omega)\, dx_0 dz_0 \;, \quad (1)$$

where $\omega = 2\pi f$ denotes the angular frequency, $\mathbf{x}_0 = [x_0\ 0\ z_0]^T$ denotes a position on the xz-plane, $\mathbf{x} = [x\ y\ z]^T$ with $y > 0$ a position within V and $\mathbf{n} = [0\ 1\ 0]^T$ the normal vector of the xz-plane. The abbreviation $\frac{\partial}{\partial \mathbf{n}}$ denotes the directional gradient in direction of the normal vector $\mathbf{n}$. For the specialized

geometry used in this paper $\frac{\partial}{\partial \mathbf{n}} P(\mathbf{x}_0, \omega)$ is given by

$$\frac{\partial}{\partial \mathbf{n}} P(\mathbf{x}_0, \omega) = \frac{\partial}{\partial y} P(\mathbf{x}, \omega)\Big|_{\mathbf{x}=\mathbf{x}_0} . \quad (2)$$

The tree-dimensional free-field Green's function $G_{0,3\mathrm{D}}(\mathbf{x}|\mathbf{x}_0, \omega)$ is given as

$$G_{0,3\mathrm{D}}(\mathbf{x}|\mathbf{x}_0, \omega) = \frac{1}{4\pi} \frac{e^{-j\frac{\omega}{c}|\mathbf{x}-\mathbf{x}_0|}}{|\mathbf{x}-\mathbf{x}_0|} , \quad (3)$$

where c denotes the speed of sound. Equation (3) can be interpreted as the pressure field generated by an acoustic point source placed at the position $\mathbf{x}_0$.
The Rayleigh integral (1) states that the pressure within V is uniquely given by integrating the weighted Green's function over the xz-plane. The weight is given by the gradient of the pressure in direction of the normal vector $\mathbf{n}$ evaluated on the xz-plane. Hence, if we aim at synthesizing the pressure of a given virtual source $S(\mathbf{x}, \omega)$ within V we can place a continuous distribution of point sources (secondary sources) on ∂V which are weighted, i.e. driven, by the directional gradient of the virtual source $\frac{\partial}{\partial \mathbf{n}} S(\mathbf{x}_0, \omega)$. The weights of the secondary sources are also termed as *driving signal* in this context.
The driving signal for the reproduction of a virtual point source located at position $\mathbf{x}_{\mathrm{ps}} = [x_{\mathrm{ps}}\ y_{\mathrm{ps}}\ z_{\mathrm{ps}}]^T$ with $y_{\mathrm{ps}} < 0$ is given as two times the directional gradient of (3)

$$D_{\mathrm{ps}}(\mathbf{x}_0, \omega) = \frac{1}{2\pi} \hat{S}_{\mathrm{ps}}(\omega) \frac{y_{\mathrm{ps}}}{|\mathbf{x}_0 - \mathbf{x}_{\mathrm{ps}}|} \times \left(\frac{1 + j\frac{\omega}{c}|\mathbf{x}_0 - \mathbf{x}_{\mathrm{ps}}|}{|\mathbf{x}_0 - \mathbf{x}_{\mathrm{ps}}|} \right) \frac{e^{-j\frac{\omega}{c}|\mathbf{x}_0 - \mathbf{x}_{\mathrm{ps}}|}}{|\mathbf{x}_0 - \mathbf{x}_{\mathrm{ps}}|} , \quad (4)$$

where $\hat{S}_{\mathrm{ps}}(\omega)$ denotes the spectrum of the virtual source (e. g. the input signal).
The same principles as outline above can also be applied to two-dimensional wave propagation scenarios. The transition from three- to two-dimensions can be performed by assuming that the field is constant in one of the coordinates [7]. Here, we will assume that the field shows no dependence in the z-coordinate. The two-dimensional equivalent of the first Rayleigh integral is then given as [7]

$$P(\mathbf{x}, \omega) = 2 \int_{-\infty}^{\infty} \frac{\partial}{\partial \mathbf{n}} P(\mathbf{x}_0, \omega)\, G_{0,2\mathrm{D}}(\mathbf{x}|\mathbf{x}_0, \omega)\, dx_0 , \quad (5)$$

where $\mathbf{x}_0 = [x_0\ 0\ 0]^T$ and $\mathbf{x} = [x\ y\ 0]^T$ with $y > 0$. The two-dimensional Green's function is given by [7]

$$G_{0,2\mathrm{D}}(\mathbf{x}|\mathbf{x}_0, \omega) = \frac{j}{4} H_0^{(2)}(\frac{\omega}{c}|\mathbf{x} - \mathbf{x}_0|) , \quad (6)$$

where $H_0^{(2)}(\cdot)$ denotes the zeroth-order Hankel function of second kind. Equation (6) can be interpreted as the pressure field generated by an acoustic line source. The driving signal for the reproduction of a virtual line source can be derived as

$$D_{\mathrm{ls}}(\mathbf{x}_0, \omega) = \frac{1}{2} \frac{j\omega}{c} \hat{S}_{\mathrm{ps}}(\omega) \frac{y_{\mathrm{ls}}}{|\mathbf{x}_0 - \mathbf{x}_{\mathrm{ls}}|} H_1^{(2)}(\frac{\omega}{c}|\mathbf{x}_0 - \mathbf{x}_{\mathrm{ls}}|) . \quad (7)$$

Equation (5) states that two-dimensional reproduction can be realized by a continuous distribution of appropriately driven line sources perpendicular to the reproduction plane. Note, that both the three-dimensional Rayleigh integral (1) and its two-dimensional variant (5) are unique. The reproduced sound field consequently matches the desired virtual source exactly within V.

2.2. 2.5-dimensional Reproduction

WFS and other sound field synthesis methods aim at the reproduction of a virtual acoustic scene in a plane only. Ideally this plane is leveled with the listeners ears. This constitutes essentially a two-dimensional reproduction scenario. From a physical point of view, according to the previous subsection, the natural choice for the characteristics of secondary sources used for two-dimensional reproduction would be line sources. However, it is desirable to use point sources as secondary sources since these can be realized in practice reasonably well by conventional loudspeakers. Using point sources as secondary sources for the reproduction in a plane results in a dimensionality mismatch, therefore such methods are often termed as *2.5-dimensional reproduction*. It is well known that 2.5-dimensional WFS suffers from artifacts [5, 8] in the reproduced sound field. Most prominent are amplitude and spectral errors in this context.
It is not straightforward to derive a driving function for 2.5-dimensional reproduction. Different techniques can be used here, resulting in different properties of the reproduced sound field. We first review

the traditional formulation of WFS in Section 3, followed by the derivation of an alternative solution using the spectral division method in Section 4.

3. WAVE FIELD SYNTHESIS

The theory of WFS has initially been developed for linear distributions of loudspeakers [6, 9] and has later on been extended to arbitrarily shaped loudspeaker distributions [10, 3]. The traditional theory of WFS is based on an approximation of the Rayleigh integral (1) to the 2.5-dimensional reproduction scenario.

3.1. Traditional Formulation

Starting point is the three-dimensional Rayleigh integral (1). This is specialized by introducing the driving function of a virtual point source as given by (4) and assuming that the virtual source and the listener are located in the xy-plane. This results in

$$P(\mathbf{x},\omega) = \frac{1}{2\pi}\hat{S}_{\mathrm{ps}}(\omega)\times \iint_{-\infty}^{\infty} \frac{y_{\mathrm{ps}}}{|\mathbf{x}_0'-\mathbf{x}_{\mathrm{ps}}|}\left(\frac{1+j\frac{\omega}{c}|\mathbf{x}_0'-\mathbf{x}_{\mathrm{ps}}|}{|\mathbf{x}_0'-\mathbf{x}_{\mathrm{ps}}|}\right)\times \frac{e^{-j\frac{\omega}{c}|\mathbf{x}_0'-\mathbf{x}_{\mathrm{ps}}|}}{|\mathbf{x}_0'-\mathbf{x}_{\mathrm{ps}}|}\;\frac{1}{4\pi}\frac{e^{-j\frac{\omega}{c}|\mathbf{x}-\mathbf{x}_0'|}}{|\mathbf{x}-\mathbf{x}_0'|}\,dz_0dx_0\;, \quad (8)$$

with $\mathbf{x}_0' = [x_0\ 0\ z_0]^T$, $\mathbf{x} = [x\ y\ 0]^T$ and $\mathbf{x}_{\mathrm{ps}} = [x_{\mathrm{ps}}\ y_{\mathrm{ps}}\ 0]^T$. The inner integral over z_0 is approximated using the stationary phase method. This method provides an approximate solution of oscillatory integrals and is linked to the method of steepest descent. We will not go into the details of calculating the approximation to (8). Refer to [5, 7] for a detailed treatment. We are rather interested in the conditions under which the method is accurate. The required condition is

$$\frac{\omega}{c}(|\mathbf{x}_0'-\mathbf{x}_{\mathrm{ps}}|+|\mathbf{x}-\mathbf{x}_0'|) \gg 1\;. \quad (9)$$

Hence, the approximation will be accurate for high frequencies and/or for large distances of the virtual source or the listener to the secondary source distribution. The approximation of the inner integral results in [5]

$$P(\mathbf{x},\omega) \approx \hat{S}_{\mathrm{ps}}(\omega)\sqrt{\frac{j\frac{\omega}{c}}{2\pi}}\int_{-\infty}^{\infty}\sqrt{\frac{|\mathbf{x}-\mathbf{x}_0|}{|\mathbf{x}_0-\mathbf{x}_{\mathrm{ps}}|+|\mathbf{x}-\mathbf{x}_0|}}\times \frac{y_{\mathrm{ps}}}{|\mathbf{x}_0-\mathbf{x}_{\mathrm{ps}}|}\frac{e^{-j\frac{\omega}{c}|\mathbf{x}_0-\mathbf{x}_{\mathrm{ps}}|}}{\sqrt{|\mathbf{x}_0-\mathbf{x}_{\mathrm{ps}}|}}\;\frac{1}{4\pi}\frac{e^{-j\frac{\omega}{c}|\mathbf{x}-\mathbf{x}_0|}}{|\mathbf{x}-\mathbf{x}_0|}\,dx_0\;, \quad (10)$$

with $\mathbf{x}_0 = [x_0\ 0\ 0]^T$. The last term in the integral can be identified as the field of a secondary point source, the remaining terms as its driving signal. However, the driving signal depends on the listener position $\mathbf{x}$, which is not desired. This dependency is removed by applying a further stationary phase approximation. The condition for this approximation is

$$\frac{\omega}{c}(|\mathbf{x}_0-\mathbf{x}_{\mathrm{ps}}|+|\mathbf{x}-\mathbf{x}_0|) \gg 1\;. \quad (11)$$

Hence, the approximation will again be accurate for high frequencies and/or for large distances of the virtual source or the listener to the secondary source distribution. However, note that the distance are measured in the xy-plane now. The second approximation results in [5]

$$P(\mathbf{x},\omega) \approx \hat{S}_{\mathrm{ps}}(\omega)\sqrt{\frac{j\frac{\omega}{c}}{2\pi}}\sqrt{\frac{y}{y-y_{\mathrm{ps}}}}\times \int_{-\infty}^{\infty}\frac{y_{\mathrm{ps}}}{|\mathbf{x}_0-\mathbf{x}_{\mathrm{ps}}|}\frac{e^{-j\frac{\omega}{c}|\mathbf{x}_0-\mathbf{x}_{\mathrm{ps}}|}}{\sqrt{|\mathbf{x}_0-\mathbf{x}_{\mathrm{ps}}|}}\frac{1}{4\pi}\frac{e^{-j\frac{\omega}{c}|\mathbf{x}-\mathbf{x}_0|}}{|\mathbf{x}-\mathbf{x}_0|}\,dx_0\;. \quad (12)$$

The strength of the secondary sources, as given by (12), depends still on the distance y of the listener to the secondary source distribution. However, this dependence turns into a constant factor under the assumption that the reproduction shall be correct on a reference line parallel to the secondary source distribution with distance y_{ref}. The traditional driving function for WFS is then given by [5]

$$D_{\mathrm{WFS}}(x_0,\omega) = \hat{S}_{\mathrm{ps}}(\omega)\sqrt{\frac{j\frac{\omega}{c}}{2\pi}}\sqrt{\frac{y_{\mathrm{ref}}}{y_{\mathrm{ref}}-y_{\mathrm{S}}}}\frac{y_{\mathrm{ps}}}{|\mathbf{x}_0-\mathbf{x}_{\mathrm{ps}}|}\frac{e^{-j\frac{\omega}{c}|\mathbf{x}_0-\mathbf{x}_{\mathrm{ps}}|}}{\sqrt{|\mathbf{x}_0-\mathbf{x}_{\mathrm{ps}}|}}\;. \quad (13)$$

3.2. The Pre-Equalization Approach

Inverse Fourier transformation of the driving signal (13) yields

$$d_{\mathrm{WFS}}(x_0,t) = s(t) * h(t) * \sqrt{\frac{y_{\mathrm{ref}}}{y_{\mathrm{ref}}-y_{\mathrm{S}}}}\,\frac{y_{\mathrm{ps}}}{|\mathbf{x}_0-\mathbf{x}_{\mathrm{ps}}|^{3/2}}\,\delta(t-\frac{|\mathbf{x}_0-\mathbf{x}_{\mathrm{ps}}|}{c}) \;, \quad (14)$$

where $*$ denotes convolution and $\delta(\cdot)$ the Dirac delta function. $h(t)$ denotes the inverse Fourier transformation

$$h(t) = \mathcal{F}^{-1}\left\{\sqrt{\frac{j\omega}{2\pi c}}\right\} \;, \quad (15)$$

which is independent from the secondary source position x_0. Hence, the driving function for traditional WFS can be computed by

- filtering the signal of the virtual source $s(t)$ with the filter $h(t)$, and
- weighting/delaying this pre-filtered signal.

This scheme is efficient with respect to computational complexity since the weighting/delay operation can be implemented by a delay line and consequently only one convolution per virtual source is required. In the context of WFS the filter $h(t)$ is termed as *pre-equalization* filter. It is evident from (15) that this pre-equalization filter is a linear-phase 3dB/Octave high-pass (HP) filter.

The driving function of traditional WFS has been derived by applying two consecutive approximations. When the assumptions underlying these approximations are not met, deviations will occur which might also have an influence on the pre-equalization filter. The focus of this paper is to investigate the constraints of the pre-equalization approach. An exact solution of the reproduction problem given by the spectral division method will be used for this purpose.

4. SPECTRAL DIVISION METHOD

The spectral division method, presented in [11, 4], utilizes a formulation of the sound reproduction problem in the spatio-temporal Fourier domain. It is applicable to planar and linear secondary point/line source distributions. It has been shown that it is equivalent to the formulation in terms of the Rayleigh integrals for two- and three-dimensional reproduction.

For the comparison with WFS we will focus on the 2.5-dimensional problem. The following section outlines the basic theory, derives the driving function for a virtual point source and links the findings to the traditional formulation of WFS.

4.1. Basic Concept

The sound field reproduced by a linear distribution of secondary point sources is given by

$$P(\mathbf{x},\omega) = \int_{-\infty}^{\infty} D(\mathbf{x}_0,\omega) G_{0,3\mathrm{D}}(\mathbf{x}-\mathbf{x}_0,\omega) dx_0 \;. \quad (16)$$

Equation (16) constitutes a spatial convolution of the driving function with the field of the secondary sources along the x-axis. Hence, the convolution theorem [12] of the Fourier transformation can be utilized. Applying a spatial Fourier transformation with respect to the x-coordinate to Eq. (16) yields

$$\tilde{P}(k_x,y,\omega) = \tilde{D}(k_x,\omega)\;\tilde{G}_{0,3\mathrm{D}}(k_x,y,\omega) \;, \quad (17)$$

where k_x denotes the wavenumber in x-direction and $\tilde{G}_{0,3\mathrm{D}}(k_x,y,\omega)$ the spatial Fourier transformation of $G_{0,3\mathrm{D}}(\mathbf{x}-\mathbf{0},\omega)$. Quantities in the spatial Fourier domain are indicated by a tilde. For sound reproduction, the reproduced sound field should match the desired sound field $P(\mathbf{x},\omega) = S(\mathbf{x},\omega)$ within the listening area. According to (17), the driving function $\tilde{D}(k_x,\omega)$ is then given as the spectral division

$$\tilde{D}(k_x,\omega) = \frac{\tilde{S}(k_x,y,\omega)}{\tilde{G}_{0,3\mathrm{D}}(k_x,y,\omega)} \;. \quad (18)$$

Hence, both the spectrum of the desired sound field and of the secondary sources have to be known.

The spatial Fourier transformation of the Green's function $G_{0,3\mathrm{D}}(\mathbf{x}-\mathbf{x}_0,\omega)$ with respect to x can be derived from [13] as

$$\tilde{G}_{0,3\mathrm{D}}(k_x,y,\omega) = \begin{cases} -\frac{j}{4}H_0^{(2)}\left(\sqrt{(\frac{\omega}{c})^2-k_x^2}\,y\right) & , \; |k_x| < \left|\frac{\omega}{c}\right| \\ \frac{1}{2\pi}K_0\left(\sqrt{k_x^2-(\frac{\omega}{c})^2}\,y\right) & , \; \left|\frac{\omega}{c}\right| < |k_x| \end{cases} \;, \quad (19)$$

where $H_0^{(2)}(\cdot)$ denotes the zero-th order Hankel function of second kind and $K_0(\cdot)$ the zero-th order modified Bessel function of second kind [14]. Note

that (19) is valid only for $y > 0$. The spectrum of the secondary sources (19) consists of two parts: a traveling contribution for $|k_x| < \left|\frac{\omega}{c}\right|$ and an evanescent contribution for $\left|\frac{\omega}{c}\right| < |k_x|$.
Evanescent waves are waves which exhibit no phase variation in at least one spatial dimension and decay exponentially in these directions [7]. They emerge from solutions of the acoustic wave equation which exhibit at least one imaginary wave number.

4.2. Derivation of Driving Function

The spatial Fourier transformation of a virtual point source (3) is required for the calculation of the driving function using (17). It can be derived in a similar way as (19) by applying suitable substitutions. It is given as

$$\tilde{S}(k_x, y, \omega) = \hat{S}_{\mathrm{ps}}(\omega) e^{j k_x x_{\mathrm{ps}}} \times \begin{cases} -\frac{j}{4} H_0^{(2)}\left(\sqrt{(\frac{\omega}{c})^2 - k_x^2}\,(y - y_{\mathrm{ps}})\right) & , \; |k_x| < \left|\frac{\omega}{c}\right| \\ \frac{1}{2\pi} K_0\left(\sqrt{k_x^2 - (\frac{\omega}{c})^2}\,(y - y_{\mathrm{ps}})\right) & , \; \left|\frac{\omega}{c}\right| < |k_x| \end{cases} , \tag{20}$$

for $y_{\mathrm{ps}} < 0$. Introducing (20) and (19) into (17) yields the driving function for the SDM. However, it is evident from (20) that the driving function depends on the distance y of the listener to the secondary source distribution. Perfect reproduction can only be achieved on a (reference) line with distance y_{ref}. Hence, the driving function for the SDM is finally given by

$$\tilde{D}_{\mathrm{SDM}}(k_x, \omega) = \hat{S}_{\mathrm{ps}}(\omega)\; e^{j k_x x_{\mathrm{ps}}} \times \times \begin{cases} \frac{H_0^{(2)}\left(\sqrt{(\frac{\omega}{c})^2 - k_x^2}\,(y_{\mathrm{ref}} - y_{\mathrm{ps}})\right)}{H_0^{(2)}\left(\sqrt{(\frac{\omega}{c})^2 - k_x^2}\, y_{\mathrm{ref}}\right)} & , \; |k_x| < \left|\frac{\omega}{c}\right| \\ \frac{K_0\left(\sqrt{k_x^2 - (\frac{\omega}{c})^2}\,(y_{\mathrm{ref}} - y_{\mathrm{ps}})\right)}{K_0\left(\sqrt{k_x^2 - (\frac{\omega}{c})^2}\, y_{\mathrm{ref}}\right)} & , \; \left|\frac{\omega}{c}\right| < |k_x| \end{cases} . \tag{21}$$

It is straightforward to show that the reproduction is perfect on the reference line, by introducing (21) together with (19) into (17). Hence, Eq. (21) provides the exact solution for 2.5-dimensional reproduction and therefore this solution can be used as a reference to evaluate WFS. The driving function of WFS (13) is not given in the spatio-temporal frequency domain. For the sake of comparison it would be desirable to derive an inverse Fourier transformation of (21). However, the analytical treatment is not straighfoward. We will show in the next section how a reasonable approximation of the driving function (21) can be used instead.

4.3. Approximation of the Driving Function

The SDM driving function (21) can be approximated by replacing the Hankel and modified Bessel function by their large-argument approximations [14]

$$\tilde{D}_{\mathrm{SDM}}(k_x, \omega) \approx \hat{S}_{\mathrm{ps}}(\omega) \sqrt{\frac{y_{\mathrm{ref}}}{y_{\mathrm{ref}} - y_{\mathrm{ps}}}} \times e^{j k_x x_{\mathrm{ps}}} \begin{cases} e^{j\sqrt{(\frac{\omega}{c})^2 - k_x^2}\, y_{\mathrm{ps}}} & , \; |k_x| < \left|\frac{\omega}{c}\right| \\ e^{\sqrt{k_x^2 - (\frac{\omega}{c})^2}\, y_{\mathrm{ps}}} & , \; \left|\frac{\omega}{c}\right| < |k_x| \end{cases} . \tag{22}$$

The approximation of the SDM driving function given by (22) holds for

$$\sqrt{\left|(\frac{\omega}{c})^2 - k_x^2\right|}\; y_{\mathrm{ref}} \gg 1 \text{ , and} \tag{23a}$$

$$\sqrt{\left|(\frac{\omega}{c})^2 - k_x^2\right|}\; (y_{\mathrm{ref}} - y_{\mathrm{ps}}) \gg 1 . \tag{23b}$$

Hence, for large distances of the reference line to the secondary source distribution ($y_{\mathrm{ref}} \gg 1$) and for large distances of the reference line to the virtual point source ($(y_{\mathrm{ref}} - y_{\mathrm{ps}}) \gg 1$). In order to understand the restrictions in terms of the temporal ω and spatial frequency k_x both the solution (21) and its approximation (22) are compared for critical parameters. Figure 2 shows the magnitude of the normalized difference between the exact and approximated driving function for a virtual source close to the secondary source distribution. The difference was normalized to the absolute value of the exact solution (21). It can be seen that the approximation of the spatio-temporal spectrum of the driving function is quite accurate.
The inverse Fourier transformation of the approximated driving function (22) can be derived as

$$D_{\mathrm{SDM}}(x_0, \omega) = \hat{S}_{\mathrm{ps}}(\omega)\; \frac{1}{2} \sqrt{\frac{y_{\mathrm{ref}}}{y_{\mathrm{ref}} - y_{\mathrm{ps}}}}\, j \frac{\omega}{c} \times \frac{y_{\mathrm{ps}}}{|\mathbf{x}_0 - \mathbf{x}_{\mathrm{ps}}|} H_1^{(2)}(\frac{\omega}{c} |\mathbf{x}_0 - \mathbf{x}_{\mathrm{ps}}|) . \tag{24}$$

Interestingly this constitutes an amplitude corrected version of the driving function for a virtual line source (7) as derived for two-dimensional reproduction based on the Rayleigh integral.
A further large-argument approximation of the Han-

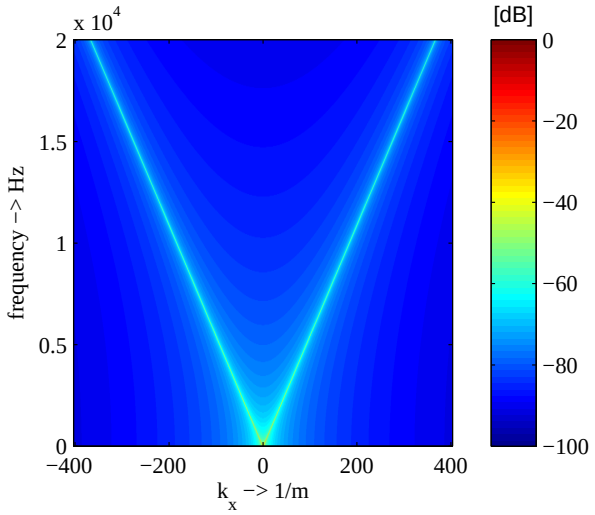

Fig. 2: Normalized difference (magnitude) between the spectrum of the exact (21) and the approximated driving function (22) ($\mathbf{x}_{\mathrm{ps}} = [0 \;\; -0.1]^T$ m, $y_{\mathrm{ref}} = 1$ m).

kel function in (24) yields

$$D_{\mathrm{SDM}}(x_0,\omega) \approx \hat{S}_{\mathrm{ps}}(\omega)\sqrt{\frac{j\frac{\omega}{c}}{2\pi}}\frac{y_{\mathrm{ps}}}{|\mathbf{x}_0-\mathbf{x}_{\mathrm{ps}}|}\sqrt{\frac{y_{\mathrm{ref}}}{y_{\mathrm{ref}}-y_{\mathrm{ps}}}}\frac{e^{-j\frac{\omega}{c}|\mathbf{x}_0-\mathbf{x}_{\mathrm{ps}}|}}{\sqrt{|\mathbf{x}_0-\mathbf{x}_{\mathrm{ps}}|}}\,, \tag{25}$$

where the condition underlying this approximation is

$$\frac{\omega}{c}\,|\mathbf{x}_0-\mathbf{x}_{\mathrm{ps}}| \gg 1\,. \tag{26}$$

Equation (25) is equal to the traditional WFS driving function (13). Hence, there is a direct link between the SDM and WFS. It can be concluded that WFS constitutes an approximation of the exact solution (21) given by the SDM. The SDM can be used as reference for WFS in order to investigate the consequences of the applied approximations.

The approximations used to derive the WFS driving function with the SDM are quite different from the ones used in WFS. The first condition (23) has shown to be quite accurate for reasonably chosen reference distances y_{ref}. The second approximation (25) is only fulfilled if the virtual point source is not too close to the secondary source distribution. Hence, it can be expected that the WFS driving function shows inaccuracies for such situations. A comparison of both approaches is presented in the next section.

5. COMPARISON OF WFS AND SDM

This section compares WFS and SDM with the aim to evaluate the effects of the approximations used in WFS. Condition (11) can be understood as a projection of condition (9) onto the xy-plane. Hence, for listeners and sources located in this plane both conditions will provide similar results. In oder to reasonably fulfill condition (11), the following requirements have to be met

1) high frequencies ω, and/or

2a) large distances of the virtual source from the secondary source distribution, or

2b) large distances of the listener (reference line) from the secondary source distribution.

The following subsection discusses the effect of the applied approximations with respect to these assumptions. The requirements 1) and 2a) are most critical in the context of sound reproduction, since 2b) can be fulfilled reasonably well when considering typical wave lengths in acoustics. We will use the approximated SDM driving function (24) as reference, since a closed form solution of the driving function is available. Remember that the applied approximation has shown to be accurate (see Fig. 2).

5.1. Reproduced Wave Field

Assuming that the listener has a reasonable distance to the secondary sources, the approximations used for the derivation of WFS will be most critical for low frequencies and virtual sources placed closely to the secondary source distribution. Figure 3 shows the synthesized sound fields for WFS and the approximated SDM driving function. A monochromatic virtual point source with a rather low frequency of $f_{\mathrm{ps}} = 200$ Hz and a position $\mathbf{x}_{\mathrm{ps}} = [0 \;\; -0.1]^T$ m close to the secondary source distribution was simulated. While the curvature of the wavefronts look correct for both methods, some slight deviations in the amplitude can be observed for WFS in Fig. 3(a). Further simulations have shown that

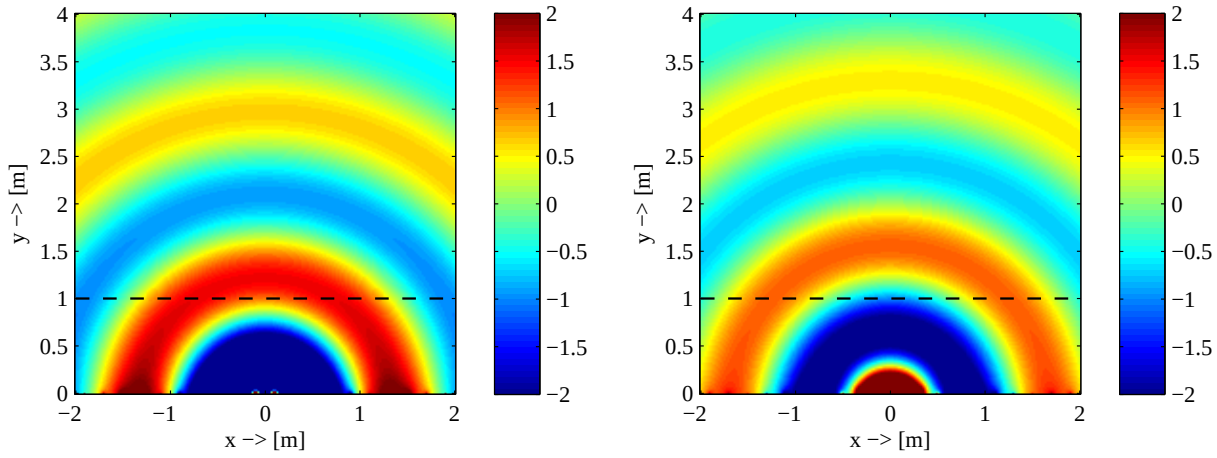

(a) WFS (b) SDM

Fig. 3: Sound field reproduced by WFS and SDM ($\mathbf{x}_{\mathrm{ps}} = [0 \ -0.1]^T$ m, $y_{\mathrm{ref}} = 1$ m, $f_{\mathrm{ps}} = 200$ Hz). The dashed line indicates the reference line.

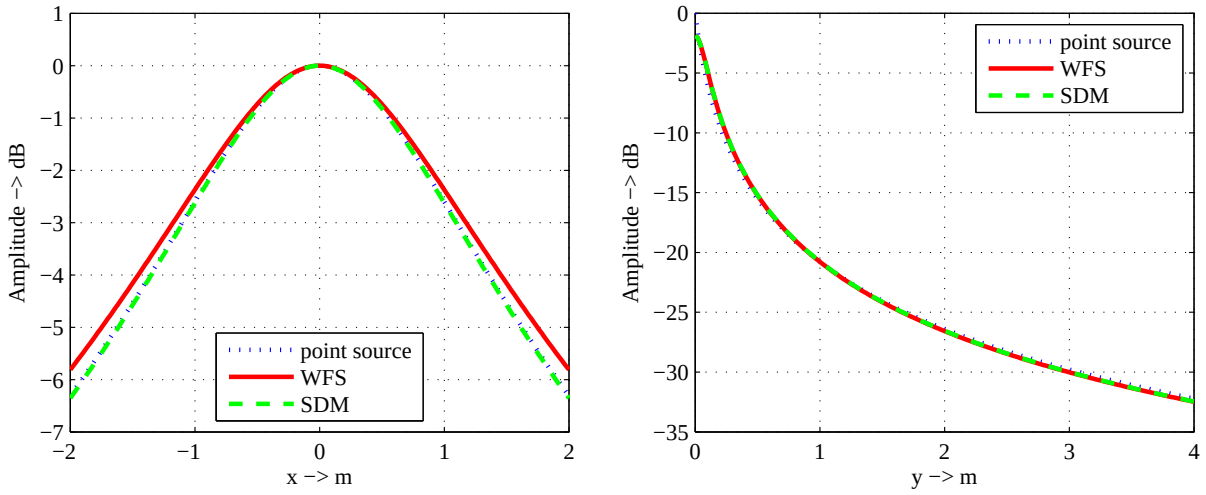

(a) along reference line ($y = y_{\mathrm{ref}}$) (b) along y-axis ($x = 0$)

Fig. 4: Amplitude distribution of WFS and SDM ($\mathbf{x}_{\mathrm{ps}} = [0 \ -0.1]^T$ m, $y_{\mathrm{ref}} = 1$ m, $f_{\mathrm{ps}} = 200$ Hz).

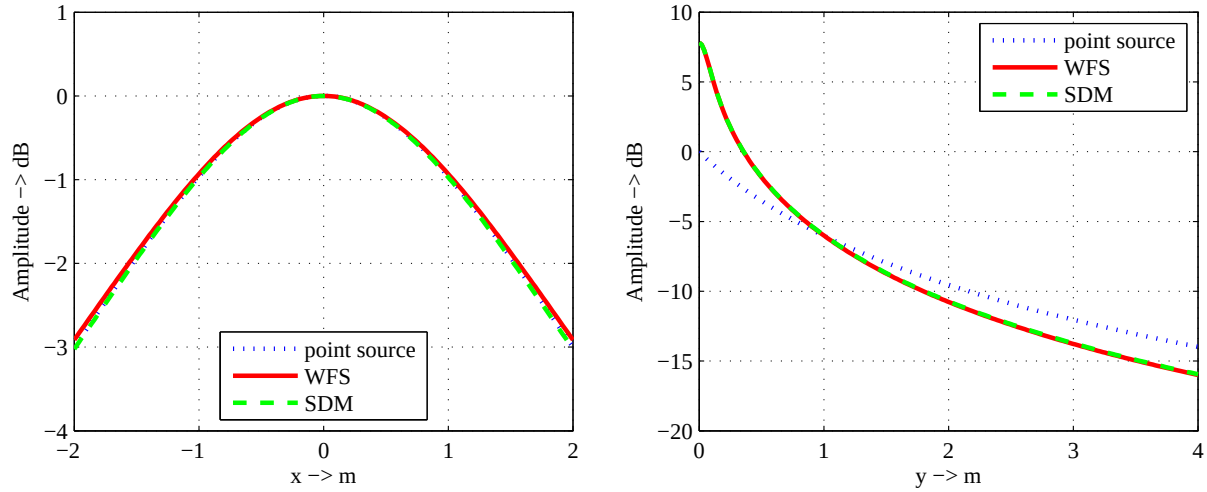

(a) along reference line ($y = y_{\text{ref}}$)

(b) along y-axis ($x = 0$)

Fig. 5: Amplitude distribution of WFS and SDM ($\mathbf{x}_{\text{ps}} = [0 \ -1]^T$ m, $y_{\text{ref}} = 1$ m, $f_{\text{ps}} = 200$ Hz).

these effects get less prominent for higher frequencies or larger distances of the virtual source to the secondary source distribution.

5.2. Amplitude Distribution

We now investigate the amplitude distribution in the reproduced sound fields. It is known that WFS and other sound reproduction methods like higher-order Ambisonics (HOA) and also the SDM show amplitude deviations for the reproduction of plane waves in 2.5-dimensional scenarios [15, 16, 4]. For WFS and SDM, as considered here, the amplitude distribution should be correct on the reference line. Figure 4 shows the amplitude distribution for WFS and SDM along the reference line and additionally along the y-axis for the situation shown in Fig. 3. WFS shows some slight deviations in the amplitude distribution along the reference line in Fig. 4(a). However, no major amplitude deviations can be observed along the y-axis. This is quite interesting since amplitude errors are present in this direction for the reproduction of a plane wave in WFS and the SDM [3, 4]. This does not seem to be case for virtual sources close to the secondary source distribution. A possible explanation is that only a short part of the secondary source distribution is driven with an considerable level. Hence, this part approximately has the characteristics of an acoustic point source.

Figure 5 shows the amplitude distributions for a virtual source position $y_{\text{ps}} = 1$ m behind the secondary source distribution, thus at a considerably larger distance from the secondary source distribution than in the scenario discussed above. Here, the amplitude distribution along the reference line is, as expected, correct for WFS and the SDM. The amplitude distribution along the y-axis shown in Fig. 5 shows the typical amplitude deviations for 2.5-dimensional reproduction. Both, WFS and the approximated SDM perform similar in this scenario. The reasons for these deviations seem to be essentially linked to the 2.5-dimensional nature of the problem.

5.3. Spectral Properties

So far, we considered the reproduction of monochromatic signals. Now, the (broadband) spectral properties of WFS in the context of its approximations is investigated. As outlined above, low frequencies and virtual sources close to the secondary source distribution are critical scenarios for the occurrence of deviations. Figure 6 shows the magnitude frequency response for a listener at position $\mathbf{x} = [0 \ 1]^T$ m in front of the virtual source placed at different distances to the secondary source distribution. The SDM has a flat frequency response for the most critical case $y_{\text{ps}} = -0.01$ m and also for all other cases

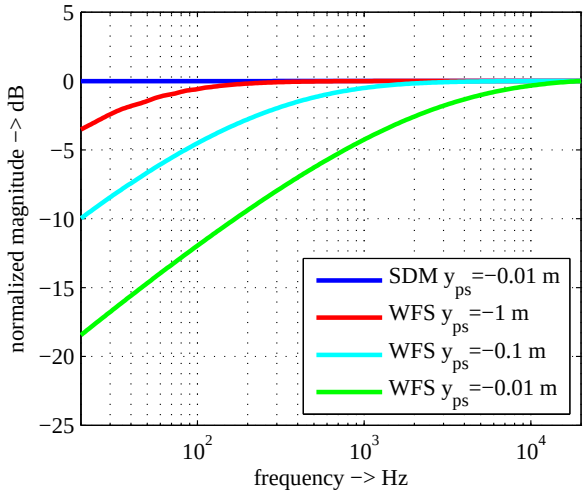

Fig. 6: Frequency response (magnitude) of the reproduced sound field at position $\mathbf{x} = [0\ 1]^T$ m for WFS and the approximated SDM driving function for different distances of the virtual source ($\mathbf{x}_{\text{ps}} = [0\ y_{\text{ps}}]^T$ m, $y_{\text{ref}} = 1$ m).

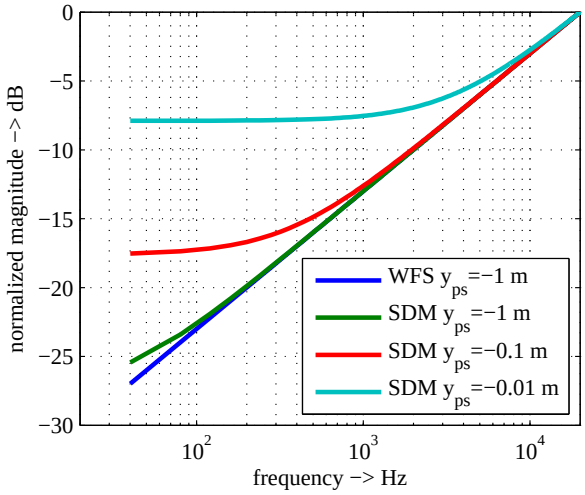

Fig. 7: Frequency response (magnitude) of the WFS and the approximated SDM driving function for different distances of the virtual source ($\mathbf{x}_{\text{ps}} = [0\ y_{\text{ps}}]^T$ m , $y_{\text{ref}} = 1$ m) for a secondary source at $x_0 = 0$ m.

shown for WFS. However, WFS shows severe deviations from the ideal frequency response. This holds especially for the close virtual source positions. The deviations degrease for increasing frequency. Both findings are in accordance with the conditions under which the approximations used for WFS hold. Note, that loudspeaker arrays are typically not used for the reproduction below about 100 Hz. Hence, the shown deviations get critical for virtual sources which are positioned closer than about 10 centimeters to the secondary source distribution.

Figure 7 shows the magnitude frequency response of the WFS and the SDM driving functions for the secondary source at $x_0 = 0$ m. The pre-equalization in the driving function for WFS (13) does not depend on the virtual source position. It has a constant high-pass character with 3dB per Octave. However, the SDM driving function shows a clear dependency on the virtual source distance to the secondary source distribution. The closer the virtual source is to the secondary source distribution the more the high-pass character is flattened out for the lower frequencies. Again the results are in accordance with the approximations used in traditional WFS.

5.4. Conclusions

The previous three subsections investigated the properties of WFS in scenarios where the approximations used in its derivation are not fulfilled. It was shown that the spatial structure of the reproduced sound field and the amplitude distribution are considerably impaired. However, the spectral properties of WFS for the synthesis of virtual sources positioned close to the secondary source distribution show severe degradations. These degradations will most likely be audible as coloration of the virtual source. The derived results might no be too critical for the synthesis of stationary virtual sources since one could take care that the positions are confined to a reasonable distance. However, the synthesis of a moving virtual source that crosses the secondary source distribution in WFS may result in unsatisfactory results. The results indicate that the pre-equalization used in WFS has to be improved in such situations in oder to avoid coloration.

6. SPATIAL SAMPLING OF SECONDARY SOURCE DISTRIBUTION

The findings presented so far were based upon the assumption of a continuous secondary source distri-

bution. In practice, the secondary source distribution is realized by loudspeakers placed at spatially discrete positions. This section reviews the influence of this spatial sampling on the reproduced sound field and draws conclusions for the pre-equalization approach as used in WFS. We will follow the theoretical framework presented in [17]. Note, the effects of sampling on the pre-equalization approach in WFS have also been discussed e. g. in [2, 18].

6.1. Spatial Sampling of Secondary Source Distribution

As for time-domain sampling, the discretization of the secondary source distribution is modeled by spatial sampling of the driving function. The sampling of the driving function $D(x,\omega)$ is described by multiplication with a series of spatial Dirac functions at the positions of the loudspeakers. For an equidistant spacing this is given by

$$D_{\mathrm{S}}(x,\omega) = D(x,\omega) \cdot \frac{1}{\Delta x} \sum_{\mu=-\infty}^{\infty} \delta(x - \Delta x \mu) \;, \quad (27)$$

where $D_{\mathrm{S}}(x,\omega)$ denotes the sampled driving function and Δx the distance between the sampling positions. These positions are indicated in Fig. 1 by the dots •. Applying a spatial Fourier transformation to (27) results in [19]

$$\tilde{D}_{\mathrm{S}}(k_x,\omega) = 2\pi \sum_{\eta=-\infty}^{\infty} \tilde{D}(k_x - \frac{2\pi}{\Delta x}\eta, \omega) \;. \quad (28)$$

Equation (28) states that the spectrum $\tilde{D}_{\mathrm{S}}(k_x,\omega)$ of the sampled driving function is given as a superposition of shifted continuous spectra $\tilde{D}(k_x - \frac{2\pi}{\Delta x}\eta, \omega)$ of the driving function. Introducing the spectrum of the sampled driving function into (17) results in the spectrum $\tilde{P}_{\mathrm{S}}(k_x, y, \omega)$ of the sound field reproduced by a spatially discrete secondary source distribution in the wavenumber domain.

$$\tilde{P}_{\mathrm{S}}(k_x, y, \omega) = 2\pi\, \tilde{G}(k_x, y, \omega) \sum_{\eta=-\infty}^{\infty} \tilde{D}(k_x - \frac{2\pi}{\Delta x}\eta, \omega) \;. \quad (29)$$

6.2. Qualitative Analysis

We consider the approximated driving function of the SDM (24) and its spatio-temporal spectrum (22) for a qualitative analysis of the influence of spatial sampling. The spatio-temporal spectrum of the secondary sources is given by (19).

Figure 8 illustrates, on a qualitative level, the construction of the spectrum of the reproduced sound field, as given by (29). The dark gray areas denote the propagating parts of the driving function $\tilde{D}_S(k_x,\omega)$ and the secondary sources $\tilde{G}(k_x,y,\omega)$, respectively, the light gray areas their evanescent contributions. Only the propagating parts of the spatio-temporal spectra of the driving function $D_{\mathrm{S}}(x,\omega)$ and the secondary sources $\tilde{G}(k_x,y,\omega)$ are bandlimited for a fixed frequency ω. The evanescent parts are not bandlimited but decay rapidly. Four different types of overlaps between the spectrum of the sampled driving function and the secondary source can be identified. It was shown in [17] that the overlaps of the spectra of the propagating contributions of the driving function and the secondary sources are the dominant contribution to the reproduced sound field. Hence, we will only consider these.

It is evident from (28) that spatial sampling may lead to spectral overlaps in the driving function and hence to spatial aliasing. The frequencies $f_{\mathrm{al},\eta}$ above which these overlaps of the propagating parts of the sampled driving function $D_{\mathrm{S}}(x,\omega)$ occur are given as

$$f_{\mathrm{al},\eta} = \eta \frac{c}{2\Delta x} \;, \quad (30)$$

where η denotes the index of the spectral overlap as given in (28). The spatial aliasing frequency f_{al} of a particular setup is given by setting $\eta = 1$. The spectral overlaps in the sampled driving function are weighted by the spectrum of the secondary sources (see Fig. 8). Consequently, the contributions which lie within the propagating parts of the spectrum of the secondary sources will be present in the reproduced sound field. This will lead to spatial sampling artifacts in the reproduced sound field if the virtual source has contributions above the spatial aliasing frequency f_{al}.

It is evident from Fig. 8 that the spectral overlaps in $D_{\mathrm{S}}(x,\omega)$ will add energy to the reproduced sound field above the spatial aliasing frequency f_{al}. This can be concluded also from Parseval's theorem [12]. This property has influence on the frequency response of a WFS system and has to be considered for the pre-equalization as discussed in the next subsection.

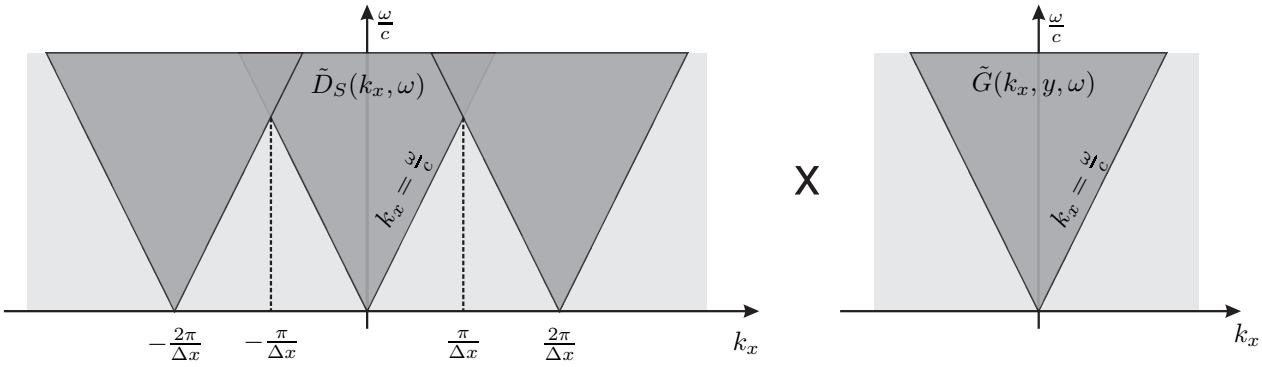

Fig. 8: Qualitative illustration of the computation of the spectrum of the reproduced sound field $\tilde{P}_S(k_x, y, \omega)$ for a sampled secondary source distribution. The dark gray areas denote the propagating parts, the light gray areas the evanescent.

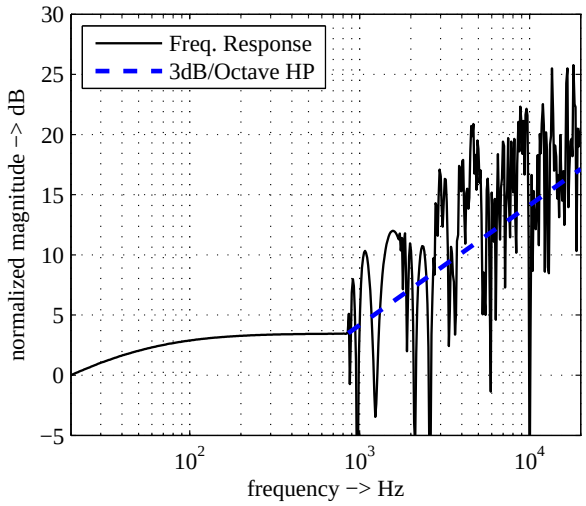

Fig. 9: Frequency response (magnitude) of the reproduced sound field at position $\mathbf{x} = [0\ 1]^T$ m for the traditional WFS driving function ($\mathbf{x}_{\text{ps}} = [0\ -1]^T$ m, $y_{\text{ref}} = 1$ m, $\Delta x = 0.20$ m).

6.3. Consequences for Pre-equalization

Figure 9 shows the frequency response of a WFS system using a spatially discrete distribution of secondary sources with a typical spacing of $\Delta x = 0.20$ m. The traditional WFS driving function (13) was used for the simulation. The spatial aliasing frequency is $f_{\text{al}} \approx 860$ Hz for the chosen setup. The increase of the magnitude response above the aliasing frequency due to the spatial sampling of the driving function is clearly visible. Figure 9 shows additionally the magnitude response of a 3dB per Octave high-pass filter starting at the spatial aliasing frequency. The increase in the magnitude response conforms roughly to this slope. Further simulations (not shown here) with smaller and larger sampling intervals Δx showed a similar HP behavior with a slope of roughly 2...4 dB per Octave depending on the parameters.

The pre-equalization in WFS compensates for the inherent low-pass (LP) character of a linear array [20] by pre-filtering with a 3dB per Octave HP filter. However, spatial sampling of the secondary source distribution adds energy above the spatial aliasing frequency. This leads approximately to a 3dB per Octave increase in the magnitude response.

It can be concluded from the above considerations and results that the pre-equalization used in WFS (and also for the approximated SDM) should only be applied below the spatial aliasing frequency of the particular setup. Above the spatial aliasing frequency less or even no pre-equalization is required. Although this result is known in the community some implementations of WFS do not cope for this fact. This results typically in strong coloration of the virtual source.

It is interesting to note, that reproduction systems like higher-order Ambisonics were the spatial bandwidth of the driving function is limited and hence no spatial aliasing occurs in the driving function do not show an HP behavior for a spatially discrete secondary source distribution [21].

7. TRUNCATION OF SECONDARY SOURCE DISTRIBUTION

Practical realizations of WFS will not only be built from spatially discrete secondary sources but also from a finite number of these. Up to now it was assumed that the secondary source distribution is of infinite length, in practice it will be of finite length. This constitutes a spatial truncation of the secondary source distribution. The influence of this truncation on the frequency response and hence the pre-equalization of WFS will be discussed in the remainder of this section. Note, similar results have also been derived e. g. in [2, 18].

7.1. Truncated Driving Function

Truncation can be modeled by multiplying the secondary source driving function $D(x_0, \omega)$ with a suitable window function $w(x_0)$ [22]

$$D_{\mathrm{tr}}(x_0, \omega) = w(x_0)\, D(x_0, \omega)\,. \tag{31}$$

A secondary source distribution with finite length L can be modeled by a rectangular window function. In this case, the window function $w(x_0)$ is given by the rect-function [12]

$$w(x) = \mathrm{rect}\left(\frac{x}{L}\right) = \begin{cases} 1 & \text{, if } |x| \leq \frac{L}{2}\,, \\ 0 & \text{, otherwise}\,, \end{cases} \tag{32}$$

for $L > 0$. Incorporating $w(x_0)$ into Eq. (16) yields the sound field $P_{\mathrm{tr}}(\mathbf{x}, \omega)$ reproduced by a truncated linear array.

Spatial Fourier transformation of (31) yields the spectrum of the truncated driving function as

$$\tilde{D}_{\mathrm{tr}}(k_x, \omega) = \frac{1}{2\pi}\, \tilde{w}(k_x) *_{k_x} \tilde{D}(k_x, \omega) \tag{33}$$

where $*_{k_x}$ denotes convolution with respect to the spatial frequency k_x and $\tilde{w}(k_x)$ the spatial Fourier transform of $w(x)$. The spatial Fourier transformation of the rectangular window $w(x)$ with respect to the x-variable is given as

$$\tilde{w}(k_x) = L\, \frac{\sin(\frac{k_x}{2}L)}{\frac{k_x}{2}L} = L\, \mathrm{sinc}(\frac{k_x}{2}L)\,. \tag{34}$$

The effects of truncation on the reproduced sound field for virtual point sources have been discussed e. g. in [17, 5]. Although an analytic solution for the synthesized sound field of a truncated driving function for a virtual point source has not been achieved so far, some general results could be derived by investigating the involved functions. These will be summarized briefly below.

The truncation of the secondary source distribution leads to a limited listening area [22, 9, 17]. The resulting listening area, for a given position of the virtual source, can be approximated quite well by simple geometric means. This approximation states that a virtual point source will be reproduced almost correctly in a wedge in front of the array which is bounded by the lines through the virtual source's position and the end-points of the secondary source distribution. Some truncation artifacts will be present within the listening area also, which can be limited by applying other window functions (tapering) to the driving function [22]. It has also been derived in [17, 23] that truncation has influence on the spatial aliasing frequency. Truncation may lead to an increased aliasing frequency.

In this paper we are interested in the effect that truncation has on the frequency response of the overall system and on the pre-equalization used in WFS. The next section will discuss this influence on a qualitative level using results from numerical simulations.

7.2. Qualitative Analysis

In order to avoid the effects of the traditional WFS driving function in the low-frequency region for nearby virtual sources (see Fig. 6) the approximated SDM driving function (24) has been used for the simulations. Furthermore, a continuous secondary source distribution and a rectangular window function $w(x)$ have been assumed. Figure 10 shows the magnitude frequency response for a listener position $\mathbf{x} = [0\ 1]^T$ m for different lengths L of the secondary source distribution. The chosen listener position is within the listening area for all chosen lengths L. It can be observed from Fig. 10 that truncation leads to an attenuation of low frequencies (HP characteristic). Especially the response for $L = 0.01$ m is almost similar to the frequency response of the SDM driving function for $y_{\mathrm{ps}} = -1$ m shown in Fig. 7. This becomes evident when considering that the chosen aperture is very close to a single secondary point source which has a flat frequency response. When increasing the length L the low frequency character-

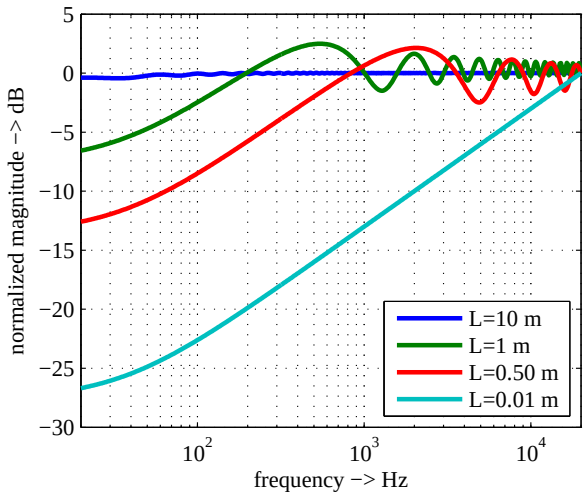

Fig. 10: Frequency response (magnitude) of the reproduced sound field at position $\mathbf{x} = [0\ 1]^T$ m for the approximated SDM driving function for different lengths L of the secondary source distribution ($\mathbf{x}_{\text{ps}} = [0\ -1]^T$ m, $y_{\text{ref}} = 1$ m).

istics for the given listener position becomes close to the desired flat frequency response. For $L = 10$ m almost no deviations can be observed. The slope of the HP is approximately 3 dB per Octave for the other lengths.

Note that the frequency response due to truncation is listener position dependent. However, within the listener area for a given virtual source position only minor deviations from the results shown in Fig. 10 will occur. Outside of the listening area further deviations besides the ones shown in Fig. 10 will be present. However, we only aim at correct reproduction within the listening area.

7.3. Consequences for Pre-equalization

The results in the previous subsection have shown that truncation has influence on the frequency response within the listening area. The results have been deduced from numerical simulations performed with the approximated driving function from the SDM. However, for virtual sources that have a reasonable distance to the secondary source distribution these results will also be valid in the context of WFS. Ideally, the transfer function from the virtual source to a listener should be flat. However, for truncated secondary source distributions the magnitude frequency response shows a more or less prominent HP character. Since this property of the transfer function is similar for listener positions within the listening area it can be corrected for by adjusting the pre-equalization filter. According to the derived results, the 3dB per Octave pre-equalization filter should only be applied in the frequency range where the frequency response of the truncated WFS system is almost flat (see Fig. 10). Unfortunately up to now no closed form solution for the sound field produced by a truncated secondary source distribution exists that could be used to determine an exact solution for the pre-equalization filter.

It is interesting to note that in WFS truncation seems to have an similar effect like virtual sources positioned close to the secondary source distribution. This can be seen when comparing figures 10 and 6. This seems to be an effect of the amplitude factor in the driving function (13). For virtual sources positioned close to the secondary source distribution most of the energy in the driving function will be concentrated to a short area of the secondary source distributions. This essentially constitutes a truncation of the secondary source distribution. However, this effect seems to be compensated for by the approximated driving function (24) of the SDM so that the resulting frequency response is flat. For WFS systems with a bend or closed secondary source contour, the secondary sources which contribute to the synthesis of a particular virtual point source have to be selected in a sensible way [24]. For moving virtual sources the active parts of the secondary source distribution might hence change over time. If the length of the active secondary source contour changes the pre-equalization has to be adapted to this situation in order to avoid coloration of the virtual source.

There is an interaction between truncation and spatial aliasing [17]. Truncation may lead to an increased spatial aliasing frequency. Hence, both truncation and spatial sampling have to be considered in the design of the pre-equalization filter.

8. CONCLUSIONS

The paper presented a detailed analysis of the pre-equalization approach used in WFS. The traditional driving signal of WFS is derived from an approximation of the first Rayleigh integral specialized to 2.5-dimensional reproduction. The approximation is

performed by applying the stationary phase method. The resulting driving signal can be split into a pre-equalization filter and a secondary source position dependent weight and delay of the pre-filtered virtual source signal. However, this solution is only accurate within the limits imposed be the assumptions used for the stationary phase method. In oder to investigate the accuracy of the traditional WFS approach an alternative solution has been used, the SDM. The SDM provides the exact solution to the 2.5-dimensional reproduction problem. The analysis of the traditional WFS approach revealed artifacts for

- low temporal frequencies, and/or
- virtual sources placed close to the secondary source distribution, and
- listeners located close to the secondary source distribution.

The artifacts that have been observed in such situations were slight deviations in the sound field (see Fig. 3(a) and Fig. 4(a)) and major deviations in the desired flat frequency response (see Fig. 6). Loudspeaker arrays are typically not used for frequencies below 100 Hz. The spectral deviations will hence become critical in terms of audible coloration for virtual sources having a distance of less than 50 cm to the secondary source distribution.
It was shown that the driving signal derived from the SDM does not exhibit these problems. However, no inverse Fourier transformation could be derived straightforwardly for the spatio-temporal spectrum of the exact solution provided by the SDM (21). It was shown that a reasonable approximation of the spatio-temporal spectrum of the driving function allows to derive an quite accurate driving function in the space-frequency domain. Interestingly, this approximated SDM driving function is the amplitude corrected driving function for two-dimensional reproduction using the Rayleigh integral. The approximated SDM driving function (24) provides the desired flat frequency response for virtual sources placed close to the secondary source distribution. Hence, this driving function can be used as an improved replacement of the traditional WFS driving function. However, efficient implementations have to be developed.

Besides the inherent limitations given by the approximations used for the derivation of WFS, two other practical issues have to be considered: spatial sampling and truncation of the secondary source distribution. It has been shown that the sampling process lead to an increase in energy for frequencies above the spatial aliasing frequency. As a consequence, the frequency response of the reproduced sound field will exhibit an high-pass character. Interestingly, this approximately results in a compensation of inherent low-pass character of a linear array. When taking this into the account, the pre-equalization filter used for WFS should at least have the following characteristics

1. 3 dB per Octave high-pass below the spatial aliasing frequency, and
2. flat frequency response above the spatial aliasing frequency.

Entirely discarding the pre-filter will result in a low-pass character below the spatial aliasing frequency of the WFS system. This typically results in a muffled sound. Applying the high-pass over the entire frequency response (discarding the flat part) will result in a high-pass character of the resulting system. It was further shown that spatial truncation of the secondary source distribution leads to a poor frequency response in the low frequency region (see Fig. 10). Regarding the typical frequency range of loudspeaker arrays, truncation will become critical for lengths $L < 0.75$ m of the secondary source distribution. Truncation leads to a HP characteristic of around 3dB per Octave. Hence, this effect could be accounted for in the pre-equalization filter by prescribing a flat frequency response for the low frequencies.
An alternative to the analytically derived pre-equalization filter is to measure or simulate the reproduced sound field of a particular setup and compute appropriate filters for the synthesis of a desired virtual source [25, 2]. Typically, databases of virtual source types and positions are constructed which are then used for the synthesis of virtual sources at any desired position. The benefit of such an approach is that most of the effects discussed above are inherently covered. The drawbacks are that the measurements are limited to a particular setup and the computational complexity. Furthermore, such methods

cannot be applied to the physically correct synthesis of moving virtual sources including the Doppler effect [26].

9. REFERENCES

[1] D. de Vries. *Wave Field Synthesis*. Audio Engineering Society, 2009.

[2] A. Apel, T. Röder, and S. Brix. Equalization of wave field synthesis systems. In *116th AES Convention*, Berlin, Germany, May 2004. Audio Engineering Society (AES).

[3] S. Spors, R. Rabenstein, and J. Ahrens. The theory of wave field synthesis revisited. In *124th AES Convention*. Audio Engineering Society (AES), May 2008.

[4] J. Ahrens and S. Spors. Sound field reproduction using planar and linear arrays of loudspeakers. *IEEE Transactions on Audio, Speech and Signal Processing*, 2010. To appear.

[5] E.N.G. Verheijen. *Sound Reproduction by Wave Field Synthesis*. PhD thesis, Delft University of Technology, 1997.

[6] A.J. Berkhout. A holographic approach to acoustic control. *Journal of the Audio Engineering Society*, 36:977–995, December 1988.

[7] E.G. Williams. *Fourier Acoustics: Sound Radiation and Nearfield Acoustical Holography*. Academic Press, 1999.

[8] J. Ahrens and S. Spors. On the secondary source type mismatch in wave field synthesis employing circular distributions of loudspeakers. In *127th AES Convention*, New York, USA, October 2009. Audio Engineering Society (AES).

[9] A.J. Berkhout, D. de Vries, and P. Vogel. Acoustic control by wave field synthesis. *Journal of the Acoustic Society of America*, 93(5):2764–2778, May 1993.

[10] E.W. Start. Application of curved arrays in wave field synthesis. In *110th AES Convention*, Copenhagen, Denmark, May 1996. Audio Engineering Society (AES).

[11] J. Ahrens and S. Spors. Reproduction of a plane-wave sound field using planar and linear arrays of loudspeakers. In *Third IEEE-EURASIP International Symposium on Control, Communications, and Signal Processing*, March 2008.

[12] B. Girod, R. Rabenstein, and A. Stenger. *Signals and Systems*. J. Wiley & Sons, 2001.

[13] I.S. Gradshteyn and I.M. Ryzhik. *Tables of Integrals, Series, and Products*. Academic Press, 2000.

[14] M. Abramowitz and I.A. Stegun. *Handbook of Mathematical Functions*. Dover Publications, 1972.

[15] J.-J. Sonke, D. de Vries, and J. Labeeuw. Variable acoustics by wave field synthesis: A closer look at amplitude effects. In *104th AES Convention*, Amsterdam, Netherlands, May 1998. Audio Engineering Society (AES).

[16] J. Ahrens and S. Spors. An analytical approach to sound field reproduction using circular and spherical loudspeaker distributions. *Acta Acustica united with Acustica*, 94(6):988–999, December 2008.

[17] S. Spors and J. Ahrens. Spatial aliasing artifacts of wave field synthesis for the reproduction of virtual point sources. In *126th AES Convention*. Audio Engineering Society (AES), May 2009.

[18] E. Corteel. *Caractérisation et Extensions de la Wave Field Synthesis en conditions réelles d'écoute*. PhD thesis, Université de Paris VI, 2006.

[19] S. Spors and R. Rabenstein. Spatial aliasing artifacts produced by linear and circular loudspeaker arrays used for wave field synthesis. In *120th AES Convention*, Paris, France, May 2006. Audio Engineering Society (AES).

[20] M.S. Ureda. Analysis of loudspeaker line arrays. *Journal of the Audio Engineering Society*, 52(5):467–495, May 2004.

[21] J. Ahrens and S. Spors. Alterations of the temporal spectrum in high-resolution sound field reproduction of different spatial bandwidths. In *126th AES Convention*, Munich, Germany, May 2009. Audio Engineering Society (AES).

[22] E.W. Start. *Direct Sound Enhancement by Wave Field Synthesis*. PhD thesis, Delft University of Technology, 1997.

[23] E. Corteel, R. Pellegrini, and C. Kuhn-Rahloff. Wave field synthesis with increased aliasing frequency. In *124th AES Convention*, Amsterdam, The Netherlands, May 2008. Audio Engineering Society (AES).

[24] S. Spors. Extension of an analytic secondary source selection criterion for wave field synthesis. In *123th AES Convention*, New York, USA, October 2007. Audio Engineering Society (AES).

[25] E. Corteel, U. Horbach, and R.S. Pellegrini. Multichannel inverse filtering of multiexciter distributed mode loudspeakers for wave field synthesis. In *112th AES Convention*, Munich, Germany, May 2002. Audio Engineering Society (AES).

[26] J. Ahrens and S. Spors. Reproduction of moving virtual sound sources with special attention to the doppler effect. In *124th AES Convention*, Amsterdam, The Netherlands, May 2008. Audio Engineering Society (AES).